

Highly Charged Ion Modified Magnetic Tunnel Junctions

Holger Grube¹, Joshua M Pomeroy¹, Andrew Perrella², John D Gillaspay¹

¹Atomic Physics Division, National Institute of Standards and Technology (NIST), Gaithersburg, Maryland, USA

²U.S. Army Research Laboratory, Adelphi, Maryland, USA; deceased

ABSTRACT

We have used highly charged ions (HCIs) such as Xe⁴⁴⁺ to modify ultrathin aluminum oxide barriers in magnetic tunnel junctions (MTJs) in order to controllably adjust their electrical properties independently of oxide thickness. We have reduced the resistance area (RA) product of our MTJ devices by up to three orders of magnitude down to our present measurement uncertainty limit of $30 \text{ } \Omega \cdot \mu\text{m}^2$ by varying the HCI dose. Preliminary experiments indicate that HCI modified Co/Al₂O₃/Co MTJs have a reduced magnetoresistance (MR) of $\approx 1 \%$ at room temperature as compared to $\approx 10 \%$ for undosed devices. The goal of this effort is to fabricate a magnetic field sensor in current-perpendicular-to-plane (CPP) geometry with an RA optimized for hard drive read heads. This is an improvement over presently demonstrated CPP architectures based on giant magnetoresistance or tunnel junctions, whose RAs are either too low or too high.

INTRODUCTION

As ever higher data densities in magnetic recording media are achieved, the conventional current-in-plane (CIP) spin valve read head can no longer be shrunk at the necessary pace. One obstacle to continued size reduction is the need for electrical isolation layers between the spin valve sensor element and the surrounding magnetic shields that are needed to maximize spatial sensitivity of the head. In read head architectures based on current perpendicular-to-plane (CPP) geometry, isolation is not necessary allowing a closer shield spacing and therefore smaller recording bit size [1]. Due to their all metal construction, CPP spin valve sensors inherently have very low impedances, which severely limits obtainable signal amplitudes [2]. The magnetoresistance (MR) $\Delta R/R_{\min}$ of typical spin valve sensors is only a few percent, but antiferromagnetically coupled multilayer structures have accomplished 65 % MR at room temperature [3]. Large sensor signals help maintain signal-to-noise ratio as magnetic bits shrink and shield gaps narrow; both are factors reducing the magnetic signal strength available for sensing, since the head fly height cannot be scaled down at the same rate. Magnetic tunnel junctions (MTJs) are CPP devices offering large MR in the tens to hundreds of percent, however, generally with high impedances [4]. Combined with the capacitance across the tunnel barrier, the resulting high RC time constant (the product of the junction's resistance R and capacitance C) limits available bandwidth, precluding high-speed data read out. The resistance area (RA) product of amorphous aluminum oxide and crystalline magnesium oxide tunnel barriers have recently been markedly reduced through process advances, although consistent fabrication of reliable ultrathin barriers is a challenge and the resulting devices are electrically fragile [1,5].

This work explores an entirely different path toward magnetoresistive CPP sensors with intermediate RA product. We fabricate MTJ devices with oxide barriers that have been modified by highly charged ion (HCI) exposure. Contrary to ions of lower charge states, which release their kinetic energy over a long path through a material, HCIs carry in addition a large amount of neutralization energy, 51 keV in the case of Xe^{44+} , which dominates their effects on surfaces. This potential energy is deposited with high intensity at the surface, leading to sputter yields of hundreds of surface atoms per individual HCI impact [6,7]. Potential energy sputtering creates nanometer sized breaches in the tunnel barriers of our devices. The size and areal density of these breaches are dependent on HCI charge state and dose, respectively [8]. We report progress toward HCI modified MTJ devices fabricated with favorable electrical characteristics, namely MR and impedance, that are between values typical for CPP spin valve sensors and MTJs.

EXPERIMENT

Metal layers are deposited by electron beam thermal evaporation in a cryo and turbo pumped ultra-high vacuum system with a base pressure lower than $3 \cdot 10^{-7}$ Pa ($2.3 \cdot 10^{-9}$ Torr) during deposition. Shadow masks define bottom and top electrode patterns with 50 μm and 60 μm line widths respectively. Substrates cut from thermally oxidized silicon (111) substrates are held near room temperature with no intentional magnetic field applied ($H < 100$ A/m ≈ 1 Oe) during deposition. A programmed quartz crystal micro balance (QCM) and a pneumatic shutter are used to automatically control film thicknesses. QCM calibration is accomplished by profilometry. Deposition rates of 0.02 nm/s for cobalt and aluminum and of 0.2 nm/s for copper are established before opening the shutter. After deposition of a uniform (no mask) adhesion layer of 0.4 nm of Co, 20 nm of Cu are deposited through a mask to define the 50 μm wide bottom lead structure and associated contact pads. A 1 nm thick uniform Co film forms the lower ferromagnetic electrode and foundation for the growth of the oxide barrier. Aluminum films are also deposited without mask and subsequently plasma oxidized in 13.3 Pa (100 mTorr) pure oxygen with a direct current of -4.5 mA applied to a 35 mm diameter stainless steel mesh held at a 20 mm distance from the sample. A mesh potential of approximately -510 V develops, while the sample is connected to the chamber ground potential. Aluminum films 0.97 nm \pm 0.05 nm thick are oxidized for 8.0 s, and 1.06 nm \pm 0.06 nm thick Al for 10.5 s. Longer oxidation times result in the loss of ferromagnetism in the underlying 1.0 nm thick Co film as determined by magnetic hysteresis loop traces, which indicate overoxidation.

HCIs from the electron beam ion trap (EBIT) facility at the National Institute of Standard and Technology are steered through a beam line into the target chamber where the aluminum oxide films are exposed. A magnetic bender separates the HCI species based on their mass-to-charge ratio m/q . Isotopically pure xenon source gas ^{136}Xe allows easy selection of a single charge state, Xe^{44+} [9,10]. HCIs are extracted at 8.2 kV electrostatic potential, which results in a kinetic energy of 360 keV for an ion with 44 elementary charges. Substrates are transported between deposition, oxidation and target chambers without breaking ultra-high vacuum.

Ion doses are calculated from a) the ion current arriving at the sample, typically 7 pA or approximately 10^6 Xe^{44+} ions per second, b) the ion beam size, about 1 mm^2 , as imaged on a beam viewer or probed with a 0.4 mm^2 aperture and c) the exposure time for the dosed device. The ion beam is smaller than the spacing of the 4 devices on a chip, which allows individual exposures of devices on a single chip, but it is also much larger than a device, ensuring uniform

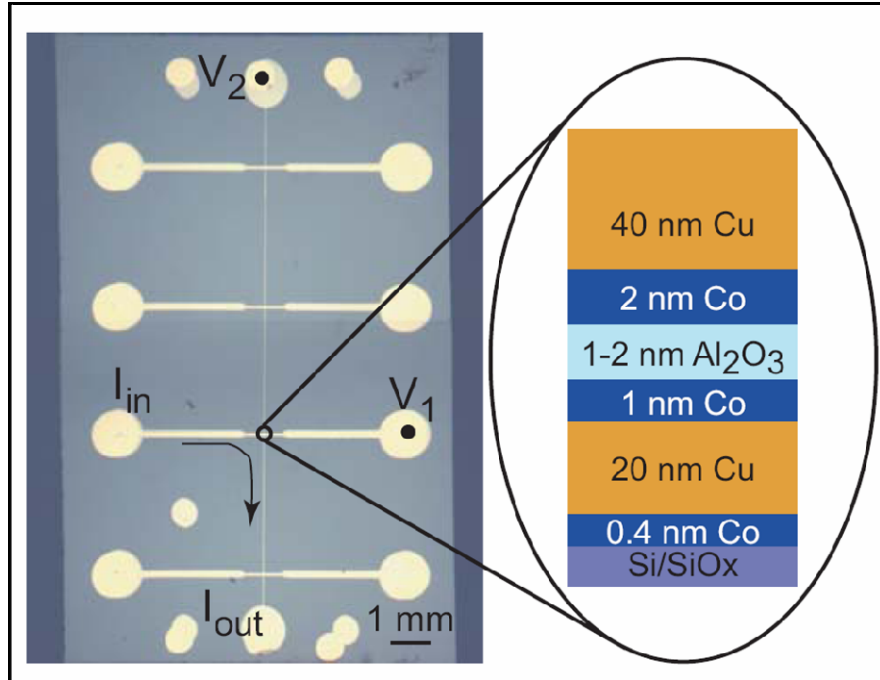


Figure 1. Left: Photo of a finished chip with four devices. In this view the bottom lead runs vertically and is crossed by four horizontal top leads. Two pads on each lead allow the devices to be measured in 4-point geometry, by supplying the current to the two device leads (at pads denoted I_{in} and I_{out}) and sensing the voltage across the tunnel barrier at the other two pads (V_1 and V_2). This is illustrated for the third device from top. Right: Layer structure in the device area, where bottom and top leads overlap. Devices are approximately $50 \mu\text{m} \times 60 \mu\text{m}$ in size.

exposure of the entire device. One device per chip is always left undosed to provide a reference impedance for the unexposed device, since the same device cannot be measured before and after exposure. The barrier oxide can only be HCI-modified before the deposition of the top leads.

Exposure is followed by evaporation of 2 nm of Co followed by 40 nm of Cu through a second mask forming the $60 \mu\text{m}$ wide top leads and contact pads. The device areas on the finished chips are defined by the intersection of the bottom and top leads, which are separated by the tunnel barrier. Both ends of each lead are accessible by pads such that the devices can be characterized with 4-point probe measurements, as illustrated in figure 1.

Since the ferromagnetic Co layers according to the above recipe are very similar, we found that they switch magnetization together, making MR measurements impossible. For MR characterizations 7 nm bottom Co leads are grown on 50 nm nickel oxide (NiO), an antiferromagnet that increases the coercivity of the bottom ferromagnetic layer. The bottom Co layer consists of 0.4 nm of uniform Co, 5.6 nm of Co deposited through mask 1 and 1 nm of uniform Co. This bottom lead structure was chosen to be most similar to the previous samples. Aluminum oxide formation and HCI modification are the same as before. Top leads consist of 4 nm of Co and 40 nm of Cu evaporated through mask 2.

A plot of the RA products of devices with the structure sketched in figure 1 that have been exposed to variable doses of Xe^{44+} ions is shown in Figure 2. The graph indicates that starting with $100 \text{ k}\Omega \cdot \mu\text{m}^2$ for the unexposed reference devices the RA product has been reduced by three orders of magnitude down to $100 \Omega \cdot \mu\text{m}^2$. In other experiments MTJs have been driven into our present measurement uncertainty limit of $30 \Omega \cdot \mu\text{m}^2$.

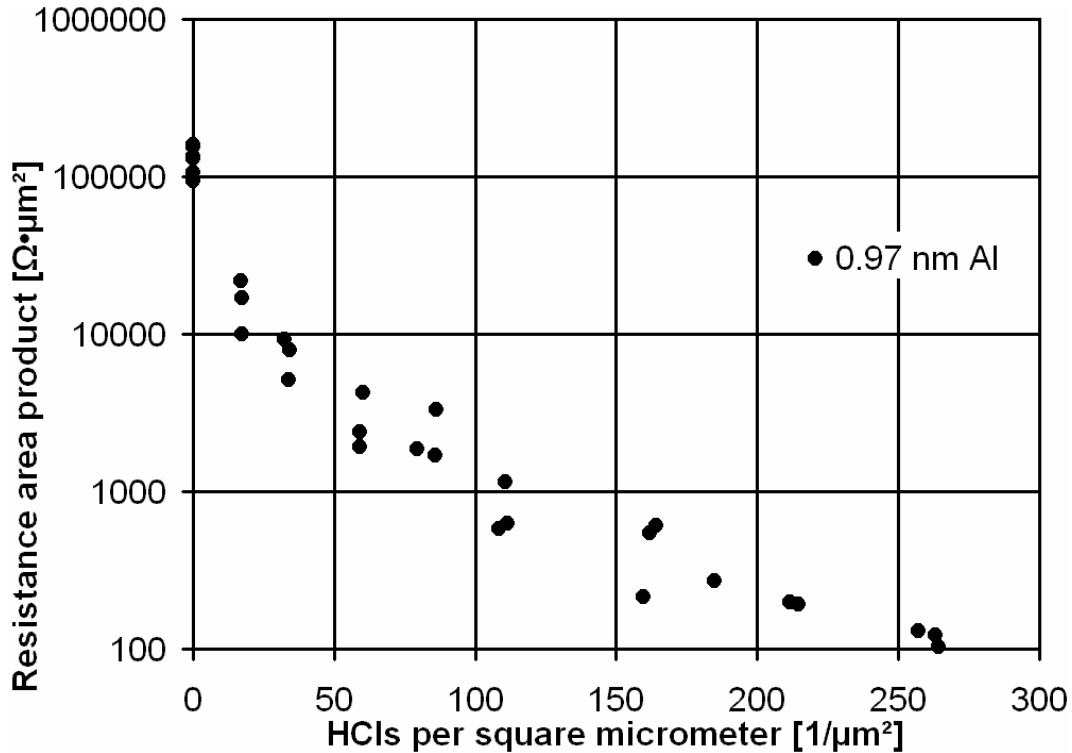


Figure 2. Plot of RA product versus HCI dose for MTJ devices according to the recipe in figure 1 with an aluminum layer thickness of 0.97 nm before oxidation. Even a dilute dose of less than 300 ions per square micrometer reduces the device impedance by three orders of magnitude.

Magnetoresistance traces for devices with a 7 nm cobalt bottom layer grown on 50 nm of NiO are shown in Figure 3. Sweeping the magnetic field between ± 12.7 kA/m (± 160 Oe) changes the resistance of an undosed device between 540 Ω and 570 Ω , corresponding to an MR of 5.75 % (left). An MR trace from a dosed device (right) on the same chip reveals a lower impedance, varying between 38.07 Ω and 38.42 Ω , but also a lower MR of 0.92 %. In a different measurement with 80 kA/m (1 kOe) available field strength the MR is measured at 8.6 % for the undosed and 1.1 % for the HCI modified device.

DISCUSSION

Experimental data shows that the RA product of MTJ devices is systematically reduced when the ultrathin oxide barrier is exposed to even dilute densities of 300 Xe^{44+} HCIs per μm^2 . The RA product dropped three orders of magnitude from a relatively high initial value of 100 $\text{k}\Omega \cdot \mu\text{m}^2$ down to 100 $\Omega \cdot \mu\text{m}^2$ as a function of the HCI dose. This demonstrates that the HCI exposure creates electrical conduction channels through the oxide, at a density directly related to the dose. Therefore by choosing a suitable HCI dose the RA value of an MTJ device can be reduced to a desired target value, for different oxide thicknesses.

MTJs with 7 nm bottom Co leads grown on an antiferromagnetic film (50 nm NiO) have also been exposed to Xe^{44+} , demonstrating the same HCI-induced reduction in RA by three orders of magnitude. Devices whose RA has been reduced by a factor of 14 compared to the corresponding control device exhibit an MR that is reduced to 0.92 % from 5.75 %. While their

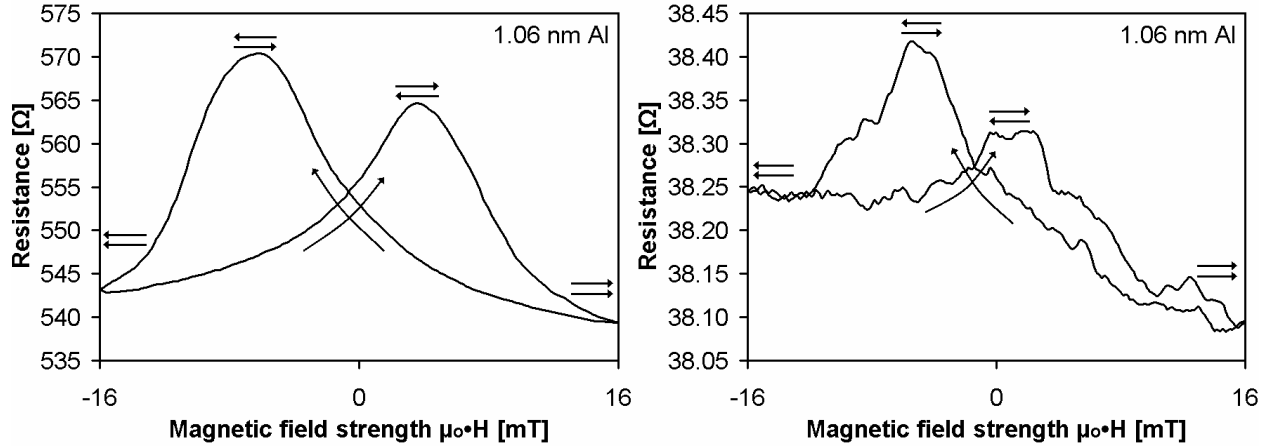


Figure 3. Magnetoresistance loops for devices with 7 nm Co bottom leads grown on 50 nm NiO to pin the lower electrode. The barrier was formed by plasma oxidation of 1.06 nm Al. The top (free) layer consists of 4 nm Co capped with 40 nm Cu. Pairs of horizontal arrows indicate layer magnetizations. The devices were cycled in a field of $\mu_0 \cdot H = \pm 16 \text{ mT}$ ($H = \pm 160 \text{ Oe}$). The cycling direction is designated by the crossed arrows. The Co films were deposited in zero magnetic field and the lower electrode has not been exchange biased by field annealing. The loop asymmetry is due to previous polarization in a higher magnetic field of 0.1 T (1 kOe). Left: The undosed control device has minimum and maximum resistances of 540 Ω and 570 Ω with an MR of 5.75 % $\Delta R/R_{\min}$. Right: The impedance of the HCI-modified device is a factor of 14 lower, varying between 38.07 Ω and 38.42 Ω , but the MR is also reduced, measuring 0.92 %.

(relative) magnetoconductance $\Delta G/G_{\min} = \Delta R/R_{\min}$ is reduced to the same value, the absolute magnetoconductance ΔG has increased from 97 μS to 239 μS . This observation is attributed to a superposition of a largely unchanged MTJ with 5.75 % MR and high RA in parallel with a small areal fraction of HCI-created conduction channels having 0.58 % MR. Given the low HCI dose and the small area each HCI affects, the barrier is mostly intact and functional. The magnitude of the MR attributed to the HCI-created channels is consistent with CPP GMR.

CONCLUSIONS

We reduced the resistance area product of magnetic tunnel junction devices using highly charged ions without varying oxide thickness. A reduction in RA by three orders of magnitude has been demonstrated. MR was seen to persist in a second generation of devices with HCI-reduced RA in a manner that implies the current shunts are magnetoresistive. Our devices and processes are not currently optimized so we anticipate progress in the near future by further lowering RA and improving MR in the modified MTJs.

ACKNOWLEDGMENTS

Funds have been provided by NIST and are gratefully acknowledged. We would like to thank Dr. Bill Egelhoff and Moshe Gurfinkel for offering advice and the use of their equipment.

REFERENCES

1. T. Kuwashima, K. Fukuda, H. Kiyono, K. Sato, T. Kagami, S. Saruki, T. Uesugi, N. Kasahara, N. Ohta, K. Nagai, et al., "Electrical Performance and Reliability of Tunnel Magnetoresistance Heads for 100-Gb/in² Application", IEEE Trans. Magn. **40**, 176 (2004).
2. K. Nagasaka, Y. Seyama, L. Varga, Y. Shimizu, and A. Tanaka, "Giant magnetoresistance properties of specular spin valve films in CPP structure," *J. Appl. Phys.* **89**, 6943 (2001).
3. S. S. P. Parkin, Z. G. Li, and David J. Smith, "Giant magnetoresistance in antiferromagnetic Co/Cu multilayers" Appl. Phys. Lett. **58** 2710 (1991).
4. J. S. Moodera, L. R. Kinder, T. M. Wong, and R. Meservey, "Large magnetoresistance at room temperature in ferromagnetic thin film tunnel junctions", Phys. Rev. Lett. **74**, 3273 (1995).
5. Y. Nagamine, H. Maehara, K. Tsunekawa, D. D. Djayaprawira, N. Watanabe, S. Yuasa, and K. Ando, "Ultralow resistance-area product of $0.4 \Omega (\mu\text{m})^2$ and high magnetoresistance above 50% in CoFeB/MgO/CoFeB magnetic tunnel junctions", Appl. Phys. Lett. **89**, 162507 (2006).
6. T. Schenkel, A. V. Hamza, A. V. Barnes, and D. H. Schneider, "Interaction of slow, very highly charged ions with surfaces", Prog. Surf. Sci. 61, **23** (1999).
7. G. Hayderer, S. Cernusca, M. Schmid, P. Varga, HP. Winter, F. Aumayr, D. Niemann, V. Hoffmann, N. Stolterfoht, C. Lemell, L. Wirtz, and J. Burgdörfer, "Kinetically Assisted Potential Sputtering of Insulators by Highly Charged Ions", Phys. Rev. Lett. **86**, 3530 (2001).
8. J. M. Pomeroy, H. Grube, A. C. Perrella, and J. D. Gillaspay, Nuclear Instruments & Methods in Physics Research Section B-Beam Interactions with Materials and Atoms (accepted 2006).
9. J. Gillaspay, "Highly charged ions", Journal of Physics B: At. Mol. Opt. Phys. **34** R93 (2001).
10. A. Pikin, C. Morgan, E. Bell, L. Ratliff, J. Gillaspay, "A beam line for highly charged ions", Reviews of Scientific Instruments **67** 2528 (1996).